Mem. S.A.It. Vol. 81, 863
© SAIt 2010
Memorie della

Advanced evolutionary phases in globular clusters.

Empirical and theoretical constraints

G. Bono[1,2]

[1] Università di Roma Tor Vergata, Dipartimento di Fisica, Via della Ricerca Scientifica, 1 00133 Rome, Italy, e-mail: bono@roma2.infn.it
[2] Istituto Nazionale di Astrofisica – Osservatorio Astronomico di Roma, Via Frascati 33, 00040 Monte Porzio Catone, Italy

Abstract. We present empirical and theoretical constraints for advanced evolutionary phases in Globular Clusters. In particular, we focus our attention on the central helium burning phases (Horizontal Branch) and on the white dwarf cooling sequence. We introduce the canonical evolutionary scenario and discuss new possible routes which can provide firm constraints on several open problems. Finally, we briefly outline new predicted near-infrared evolutionary features of the white dwarf cooling sequences which can be adopted to constrain their evolutionary properties.

Key words. Stars: photometry – Stars: evolution – Stars: Population II – Galaxy: globular clusters

1. Introduction

Globular clusters (GCs) and their stellar content played a fundamental role in the development of Stellar Astrophysics (Sandage 1953). The discovery of different stellar populations (Baade 1958), resulted in a revolutionary change in the size and age of the universe (Osterbrock 2003). Moreover, GCs were adopted to estimate the distance of the solar system from the Galactic center (Shapley 1928), and also to constrain the formation and evolution of the Milky Way spheroid (Eggen et al. 1962; Zinn 1985).

The reader interested in a detailed historical and scientific summaries of the significant theoretical and empirical progresses made by Stellar Astrophysics during the fifties and the beginning of the sixties is referred to The Vatican Conference (O'Connell 1958), to the series of *grey books*, namely *Galactic Astronomy* (Blaauw & Schmidt 1965); *Stellar atmospheres* (Greenstein 1965); and *Stellar Structure* (Aller & McLaughlin 1965). More recent reviews for North American scholars and institutions have been given by (Sandage 2007) and for the European ones by (Blaauw 1999, 2004).

During the early fifties, photometric (Sandage 1953; Arp 1955) and spectroscopic (Wallerstein 1958; Kraft 2009) data and, in particular, the comparison with early evolutionary computations (Schwarzschild et al.

Send offprint requests to: G. Bono

1957; Hoyle 1959) supported the evidence that the stellar content of GCs is coeval and chemically homogeneous. This suggests that GCs can provide independent estimates of two cosmological parameters: a lower limit to the age of the Universe (t_0) and an upper limit to the primordial helium content (Iben & Rood 1969; Buzzoni et al. 1983).

These outstanding results were supplemented during the eighties with the use of CCD cameras from the observational point of view and with detailed evolutionary tracks covering the hydrogen and the He burning phases. These new facilities provided the opportunity to detect white dwarfs (WD) in GCs (Richer & Fahlman 1988; Ortolani & Rosino 1987; Moehler et al. 2007) together with accurate and complete CMDs reaching several magnitudes below the turn-off region. However, the significant improvement in photometric accuracy and completeness was provided by HST. During the nineties, the detection of sizable samples of cluster WDs was possible (Cool et al. 1996) and these detections approached the limit of H-burning structures (King et al. 1998). Obviously, the progress made in the understanding of the evolutionary properties of low-mass stars swept across a significant improvement in the input physics: opacity, (Iglesias & Rogers 1996; Potekhin et al. 1999; Ferguson et al. 2005); equation of state (Rogers & Nayfonov 2002); cross sections (Angulo et al. 1999); and in the physical assumptions: gravitational settling, (Thoul et al. 1994; Cassisi et al. 1999; Schlattl & Salaris 2003; Michaud et al. 2004); mixing, (Chiosi & Maeder 1986; Ventura et al. 1998; VandenBerg et al. 2006; Charbonnel & Lagarde 2010); mass loss, (Chiosi et al. 1992; Vink & Cassisi 2002; Ventura & Marigo 2010); outer boundary conditions, (Cassisi et al. 2000; VandenBerg et al. 2008) adopted to construct stellar evolutionary models.

During the last ten years, this paramount effort was extended to include either broken regions such as the Galactic bulge (Zoccali et al. 2000, 2003) or advanced evolutionary phases: Extreme HB stars, (EHB, Moehler et al. 2004b; Heber 2009); AGB, (Marigo & Girardi 2007; Marigo et al. 2008; Weiss & Ferguson 2009); WD cooling sequences, (Calamida et al. 2008; Kalirai et al. 2008; Strickler et al. 2009; Althaus 2010a; Salaris et al. 2010) or exotic phenomena (Strassmeier et al. 2010), or new physical mechanisms, such as stellar rotation (Maeder & Meynet 2000) and more sophisticated mixing mechanisms (Penev et al. 2009).

Recently, deep HST photometry disclosed the presence of multiple stellar populations in several massive GCs. Together with the most massive Galactic globular ω Centauri (Anderson 2002; Bedin et al. 2004) multiple stellar sequences have been detected in GCs covering a broad range of metal content: NGC 2808 (D'Antona et al. 2005; Piotto et al. 2007), M54 (Siegel et al. 2007) and NGC 1851 (Calamida et al. 2007; Milone et al. 2008). Some of these multiple sequences (ω Cen, NGC 2808, NGC 1851) might be explained either with a He-enhanced (Norris 2004; D'Antona et al. 2005; D'Antona & Caloi 2008; Piotto et al. 2007), or with a CNO-enhanced (Calamida et al. 2007; Cassisi et al. 2008) sub-population. However, no general consensus has been reached concerning the physcal mechanisms, the evolutionary history and the fraction of these stellar components.

The structure of this paper is the following. In §2 we will discuss some intrinsic properties of GCs which make them perfect laboratories to constrain the physical mechanisms and the leading parameters governing their evolution. The evolutionary properties of Horizontal Branch stars is discussed in §3, while §4 deals with white dwarf cooling sequences. Finally, in §5 we briefly outline future possible avenues concerning advanced evolutionary phases in GCs.

2. De utilitate globular clusters

Some of the positive features in dealing with the stellar content of GCs have already been mentioned in the above section. Here we would like to mention a few other positive features, typically adopted in comparing theory and observations in GCs. One of the main reasons

why GCs are a crucial stellar benchmark is because they are *redundant systems*. There are four major forms of redundancy in GCs:

- **Time redundancy** –
  The distribution of cluster low-mass stars along the Main Sequence (MS) depends on the actual value of stellar mass. Data plotted in Fig. 1 show the optical V,V-I CMD of the globular NGC3201 (Bono et al. 2010). Data along the MS were collected with ACS-WFC at HST and according to the adopted set of stellar isochrones the stellar masses range from $0.25 M_{\odot}$ at V~25 and V-I~2 mag to 0.79 $M_{\odot}$ in the Turn-Off (TO) region (at V~18.2; V-I~0.92 mag). The TO region is the evolutionary phase with the largest stellar mass, since during the subsequent evolutionary phases the structures start to loose a fraction of their envelope via stellar winds. A conservative estimate of the age of typical GCs gives 12±2 Gyr; therefore, they are among the oldest stellar systems in the Galaxy and in the universe. This means that they host the evolutionary relics of all the stars with stellar masses larger than the actual TO mass. This applies not only to the progeny of low- and intermediate-mass stars which end up their evolution as CO-core WDs (WD cooling sequences, see Fig. 1), but also to massive stars which end up their evolution as core-collapse supernovae (neutron stars, stellar mass black holes) and of binary evolution (Low-Mass X-Ray Binaries, Blue Stragglers, He-core WDs, low-mass CO-core WDs). The crucial consequence of this *evolutionary continuum* is that either a physical mechanism (gravitational settling) or a chemical anomaly (abundance anti-correlations), or binarity affecting current un-evolved MS stars has already left its fingerprint in more-massive stellar structures. In principle, we can investigate *in situ* the impact which the quoted mechanisms and peculiarities have had either on advanced evolutionary phases (Red Giant Branch [RGB], Horizontal Branch [HB], Asymptotic Giant Branch [AGB], WD) or on the relics of more-massive cluster stars.
- **Internal redundancy** –
  Cluster stars present an intrinsic redundancy and indeed the ratio between the number of stars located across the TO region and subsequent evolutionary phases (SGB, RGB, HB, AGB, bright portion of the WD cooling sequence) only depends on their evolutionary lifetimes. The same ratio between two MS regions located below the MSTO do depend on both the evolutionary lifetime and on the Initial Mass Function (IMF). The difference is mainly due to the fact that in the latter case we are dealing with evolutionary phases characterized by different mean mass values. These features bring forward two relevant consequences: *i)*– star count ratios between the MSTO and more evolved evolutionary phases can be easily compared with evolutionary lifetimes; *ii)*– low- and very-low mass stars can be adopted to constrain the present day mass function (Marks & Kroupa 2010). The observational uncertainties in these comparisons are only dominated by statistics, and in turn, by the total luminosity of the cluster (Castellani et al. 2007). It is also worth noting that the total number number of stars in a specific evolutionary phase does depend on the evolutionary lifetime and on the total luminosity of the cluster. This is the reason why fast evolutionary phases or exotic objects can be easily either traced or identified in more massive clusters (47 Tuc, ω Cen, Thompson et al. 2010; Randall, Calamida & Bono 2009).
- **External redundancy** –
  Galaxies of all morphological type host GCs. Their number ranges from a few in dwarf galaxies (four in Fornax dSph, Buonanno et al. 1998) to a few hundreds in large spirals: ~200 in the MW (Harris 1996) and ≈400 in M31 (Galleti et al. 2004) to a few thousands in giant ellipticals (Harris 2009, and references therein). The luminosity function of GCs is a robust secondary distance indicator (Di Criscienzo et al. 2006) which provides accurate distances up to 100Mpc (Coma cluster, Woodworth & Harris 1992). Moreover, the integrated colors and

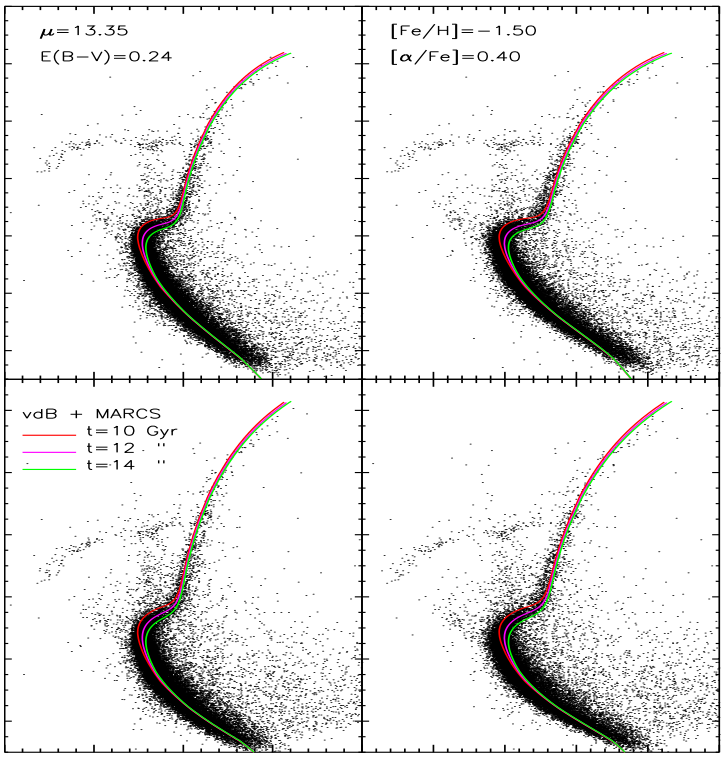

Fig. 2. Top – From left to right, V,V-J and I,V-K CMDs of NGC 3201. The colored lines show the same isochrones plotted in Fig. 1. The distance modulus, the reddening and the chemical composition adopted to compare theory and observations are labeled. Bottom – same as the top, but for the I,V-J and I,V-K CMDs.

spectrophotometric properties provide key information on the stellar content in the local (bulge/halo GCs) and in the nearby Universe.

– **Wavelength redundancy** –
Astrophysical sources typically emit in different wavelength regions, but only a few stellar systems host objects emitting from the radio (millisecond pulsars Freire et al. 2005), to the mid-infrared (AGB, Novae, Boyer et al. 2009), near-infrared (AGB, RG Valenti et al. 2007), optical (CMD, radial and non radial variables, Albrow et al. 2001), near-UV (extreme HB stars, Iannicola et al. 2009), far-UV (extreme HB stars, bright WDs, Dieball et al. 2007), X-ray (low-mass X-Ray binaries, Heinke 2010) and γ-ray (millisecond pulsars, Anderhub et al. 2009; Abdo et al. 2010; Lee et al. 2010).
The main advantage of this positive feature is that from γ-Ray to radio we often deal with multiple realizations of the same stellar system. This means that the same predictions (evolutionary models, isochrones, luminosity functions) once transformed into the observational plane, should provide, within the uncertainties affecting the photometry and the reddening law (Bono et al. 2010), the same intrinsic properties. Data plotted in Fig. 2 show the stellar content of NGC 3201 when moving from the optical to the NIR bands. This multi-wavelength approach has be-

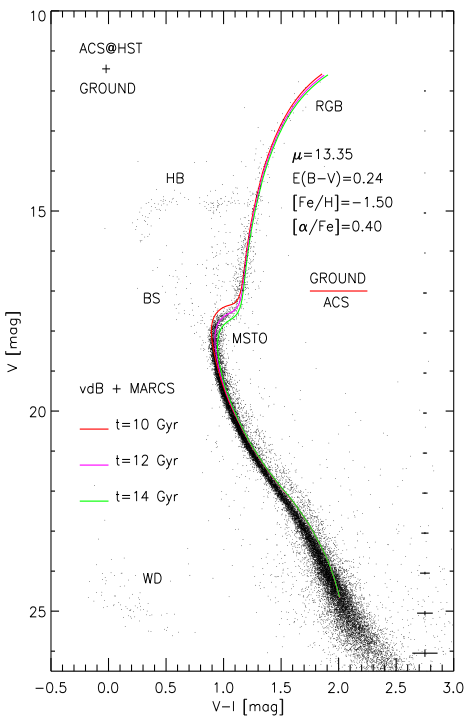

Fig. 1. Optical V,V-I CMD of the globular NGC 3201 based on data collected with space (HST) and ground-based telescopes (Bono et al. 2010). The most relevant evolutionary phases are labeled: MSTO (main sequence turn-off), BS (blue stragglers), RGB (red giant branch), HB (horizontal branch), WD (white dwarfs). The colored lines display three different cluster isochrones (VandenBerg, Casagrande & Stetson 2010) at fixed chemical composition. The adopted distance modulus, reddening, iron and α-element abundances are also labeled.

come more popular in the last few years, thanks to space and ground-based telescopes. The key advantage of this approach is to investigate the properties of the same stellar structures, by using a broad wavelength coverage, and to single out the possible occurrence either of thorny systematic errors in the absolute calibration of the data, or in the reddening correction, or in the photometric reduction strategy.

3. The Horizontal Branch

The evolutionary properties of HB stars have already been discussed in a large number of observational and theoretical investigations (e.g., Moehler 2010, and references therein). In the following, we briefly summarize the evolutionary properties relevant in tracing the transitions from the HB to the WD cooling sequence. The key parameter to explain the stellar distribution along the Zero-Age-Horizontal Branch (ZAHB) is the total mass. The mass of the He-core in low-mass stars is, at fixed chemical composition, quite constant over a broad age range. Therefore, lower mass HB structures are characterized by lower envelope masses and hotter effective temperatures (bluer colors). According to the effective temperature/color, the HB structures can be split into three different groups: EHB stars (T_e > 20,000 K), Blue (hot/warm) HB stars (BHB, 6,000 < T_e < 20,000 < K) and red (cool) HB stars (RHB, T_e < 6,000 K). The quoted groups are characterized by different final evolutionary fates during the off-ZAHB evolution. In the recent literature, several new hypotheses have been suggested to account for some features of HB stars in GCs (Catelan 2009).

In particular, to explain why the position of a fraction of EHB stars that at fixed color attain slightly fainter magnitudes, the *hot helium-flasher* scenario was suggested by Castellani et al. (1993), but see also D'Cruz et al. (1996), Brown et al. (2001, 2010) and Castellani et al. (2006). Such an evolutionary channel predicts that red giant stars undergoing violent mass-loss events approach the tip of the red giant branch with a total mass that is too small for removing the electron degeneracy of the helium core, and in turn for central helium ignition. These stellar structures leave the red giant branch and move toward their helium-core white dwarf cooling sequence. During these evolutionary phases, the hydrogen shell is still active, and the mass of the helium core is steadily increasing. Evolutionary prescriptions suggest that the structures with a helium-core mass slightly larger than this limit undergo a helium-core flash at high temperatures, ei-

ther during their approach to the white dwarf cooling sequence (*early hot helium flasher*, Castellani et al. 1993; D'Cruz et al. 1996), or along this sequence (*late hot helium flasher*, Brown et al. 2001).

This evolutionary scenario is also predicting that a globular cluster hosting a large number of *hot helium-flashers* should also be affected by a deficit in RGs, and host a significant number of helium-core white dwarfs. The final fate of the red giants with a helium-core mass smaller than the limit for central helium ignition is, indeed, as a helium-core WD (Castellani et al. 2006). This scenario has been supported by empirical evidence. A deficit of the order of 20% in the number of bright RGB stars in the globular cluster NGC 2808 from HST photometry was found by Sandquist & Martel (2007). Moreover, Calamida et al. (2008), found that the GC ω Centauri hosts a fraction of He-core white dwarfs ranging from 10% to 80%, depending on their mean mass. The quoted findings suggest that candidate helium-core white dwarfs are typically identified in stellar clusters showing well defined blue HB tails, like the metal-rich old open cluster NGC 6791, the globular clusters ω Cen and NGC 6397 (Strickler et al. 2009). The reader interested in a detailed discussion concerning the mix of candidate *hot helium flashers* and candidate helium-enriched EHB stars in ω Centauri is referred to Cassisi et al. (2009), and to Brown et al. (2010).

The HB models plotted in Fig. 3 show the evolution of selected canonical HB models. The evolutionary prescriptions plotted in this figure and in the next ones have been provided by Pietrinferni et al. (2004, 2006)[1]. The EHB structures are the low-mass tail of HB stars and a significant fraction of them, after central He exhaustion, evolve toward higher luminosity and hotter effective temperatures. Thus, they do not experience an asymptotic giant phase, since they do not evolve toward their Hayashi track. They are the so-called AGB Manque' stars (see solid lines in Fig. 3, Greggio & Renzini 1990).

[1] See also http://www.oa-teramo.inaf.it/BASTI

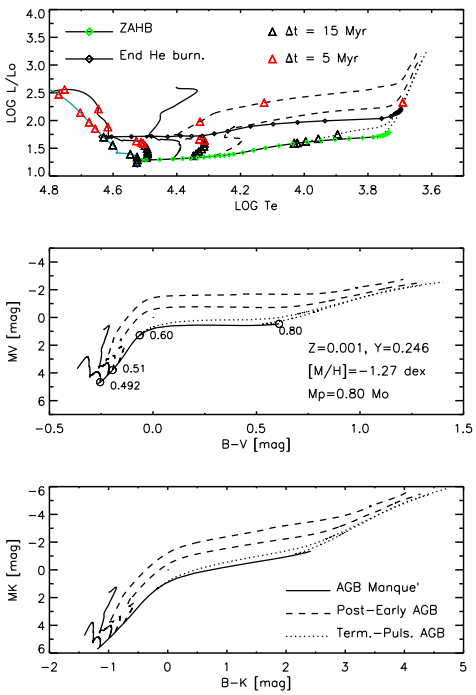

Fig. 3. Top – HR diagram of HB models constructed at fixed alpha-enhanced chemical composition and for a broad range of stellar masses. The mass of the progenitor is $0.80 M_{\odot}$ and its age is 12 Gyr. The almost horizontal lines show the ZAHB (green circles) and the central helium exhaustion (black circles). The solid lines display the evolution of low-mass AGB Manque' structures, the dashed lines the evolution of Post Early AGB structures, while the dotted lines the evolution of Thermal Pulsing AGB. The solid cyano line shows the evolution of a *hot helium flasher* computed assuming a similar composition ([M/H]=-1.1 dex; Y=0.23) and a mass value of M=0.49 $M_{\odot}$. The black triangles mark along selected HB models steps of 15 Myr, while the red ones steps of 5 Myr after 100 Myr of evolutionary lifetime. Middle – Same as the top one, but the models were transformed into the observational plane (M_V, B-V). The HB mass (solar units) of selected models are labeled. Bottom – Same as the top, but for an optical-NIR CMD (M_K, B-K).

The solid cyano line plotted in Fig. 3 shows the HB evolution of a *hot helium flasher* constructed by assuming a similar chemical com-

position ([M/H]=-1.1 dex, Y=0.23) and mass value of M=0.49$M_{\odot}$ (Cassisi et al. 2003). The ZAHB position of this model is, as expected, fainter than the canonical one, but both the central helium burning phases and the AGB Manque' phase are similar to the canonical one.

The BHB structures have intermediate-mass values among HB stars. Their distinctive evolutionary feature is that soon after central He exhaustion, they ignite He in a shell, and in turn their AGB phase starts (double shell burning) in the hot region of the HR diagram. They do not experience thermal shell flashes and have been called Post-Early-AGB (PEAGB, see dashed lines, in Fig. 3, Greggio & Renzini 1990).

The RHB structures are the high mass tail of HB stars, and their ZAHB location is between the RR Lyrae instability strip and the cool side of the HB region. They evolve almost at constant effective temperature and start their AGB phase almost at fixed luminosity and effective temperature (AGB Bump). The occurrence of this evolutionary feature marks the ignition of helium-burning in a shell. These structures experience a number of helium-shell flashes, during which they cross the Mira instability strip, the OH-IR region, to become, at the end of this phase, planetary nebulae (Wood et al. 1992). The solid dotted lines in Fig. 3 display their off-ZAHB evolution. Between the BHB and the RHB region, the HB stars are pulsationally stable and form the instability strip of RR Lyrae stars (Bono et al. 1997).

3.1. He-enhanced HB models

The possible occurrence of He-enriched stars in GCs dates back to the sixties (Iben & Rood 1969). During the last few years, it has become quite popular to explain either the blue tails of the HB (D'Antona & Caloi 2008), or the presence of multiple sequences in GCs (Piotto et al. 2007). The presence of He-enriched stars in GCs seems to be connected with the occurrence of well defined anticorrelations and star-to-star abundance variations. Spectroscopic measurements of cluster RG stars showed the presence of star-to-star variations not only in C, N and Na (Osborn 1971; Cohen 1978; Peterson 1980), but also in Al and in O (Norris et al. 1981; Pilachowski, Sneden & Wallerstein 1983; Leep, Wallerstein, & Oke 1986) abundances in many GGCs. The observational scenario was further enriched by the evidence that the molecular band-strengths of CN and CH seem to be anticorrelated (Smith 1987; Kraft 1994). More recently, the quoted anticorrelation together with the anticorrelations between O–Na and Mg–Al have been observed in evolved (red giant branch, Horizontal Branch), and in unevolved MS stars of a significant fraction of GC investigated (Suntzeff & Smith 1991; Cannon et al. 1998; Harbeck, Grebel & Smith 2003; Gratton et al. 2001; Gratton, Sneden & Carretta 2004; Ramirez & Cohen 2002; Carretta et al. 2007).

To explain these observations, it was suggested that a previous generation (first generation) of asymptotic giant branch (AGB) stars expelled processed material during thermal pulses, and the subsequent stellar generation (second generation) formed with contaminated material (Ventura et al. 2001). In this scenario, the surface abundances of the second stellar generation show a significant He enrichment and well defined CN and ONa anticorrelations. It was suggested that the fraction of stars belonging to the second generation might be of the order of 50% (D'Antona & Caloi 2008; Carretta et al. 2009). The key difficulty in the validation of this working hypothesis is that helium absorption lines in the visible spectral region appear at effective temperatures hotter than 10,000 K (Behr 2003,?; Moehler et al. 2004b). These effective temperatures in a GC are typical of hot and extreme HB stars. However, their helium abundances cannot be adopted to constrain the original helium content, since gravitational settling and/or radiative levitation affect their surface abundances. In a recent investigation (Villanova et al. 2009) identified helium absorption lines in a few warm cluster HB stars that should be marginally affected by the quoted mechanisms, but the range in effective temperature seems very narrow.

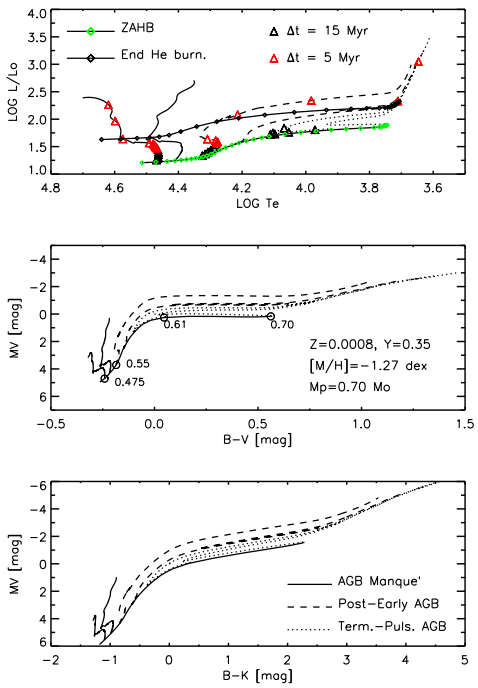

Fig. 4. Same as Fig. 3, but for HB models constructed assuming the same global metallicity, ([M/H]=-1.27 dex), but a helium enriched composition (0.35 vs 0.246). The mass of the progenitor is 0.70 $M_{\odot}$ and its age is 12 Gyr.

According to alternative working hypotheses, the cluster self-pollution is caused either by evolved RGB stars that experienced extra-deep mixing (Denissenkov & Weiss 2004), or by fast rotating intermediate-mass stars (Maeder & Meynet 2000; Maeder & Meynet 2006; Prantzos & Charbonnel 2006; Decressin et al. 2007). In the recent literature, there is a lively debate concerning the role played by the different polluters. The interested reader is referred to Renzini (2008) and to Shen et al. (2010).

The presence of a He-enriched subpopulation also accounts for the occurrence of Hot and Extreme HB stars. Evolutionary prescriptions indicate that He-enriched structures, at fixed metal abundance and cluster age, have a smaller Turn-Off mass when compared with structures constructed by assuming canonical helium content. Therefore, a He-enriched subpopulation, for a fixed mass loss rate, is characterized by smaller envelope masses, and therefore they will mainly populate the hot and the extreme region of the HB (Bono et al. 1995). Thus, the presence of a He-enriched sub-population alleviates the need of significant changes in the mass-loss efficiency along the red giant branch, required by the canonical scenario to populate the EHB region.

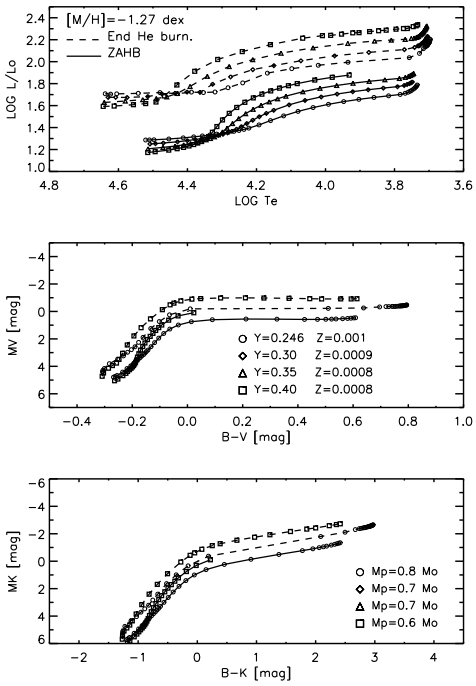

Fig. 5. Top – HR diagram showing ZAHBs (solid lines) and exhaustion of central Helium burning (dashed lines) for different sets of HB models constructed assuming an α-enhanced mixture, at fixed global metallicity ([M/H]=-1.27 dex) and different helium contents (see labeled values). Middle – Same as the top, but transformed into the observational plane (M_V, B-V) and only for the canonical and the most helium-rich HB models. Bottom – Same as the top, but for an optical-NIR CMD (M_K, B-K).

In this theoretical framework, the HB morphology is governed by two parameters, namely the metal and the helium content. This topic has been the crossroads of several theoretical and empirical investigations. In the following, we briefly outline the evolutionary properties of He-enriched HB structures. Fig. 4 shows a set of HB models computed by assuming a α-enhanced mixture and a He-enriched composition. The above models, when compared with canonical HB models plotted in Fig. 3, have the same global metallicity ([M/H]=-1.27 dex) and the same age of the progenitor (12 Gyr), but the mass of the progenitor is smaller (0.70 vs 0.80 $M_{\odot}$). The HB models plotted in Fig. 3 and in Fig. 4 display, on average, the same evolutionary features. Canonical and He-enriched HB models cover the same range of luminosities and effective temperatures. The similarity applies not only to the HR diagram, but also to the optical (middle panels) and to the optical-NIR (bottom panels) CMDs.

In order to further constrain this key point, Fig. 5 shows evolutionary prescriptions for different sets of ZAHBs and central helium exhaustion models computed by assuming the same global metallicity and a very broad range of helium contents (see labeled values). HB models plotted in the middle and in the bottom panel indicate that the difference in magnitude, at fixed color, is at most of the order of a few tenths of a magnitude. The difference in color, at fixed magnitude, is smaller even in the M_K, B-K CMD. This evidence suggests that uncertainties either in distance moduls or in reddening hamper the comparison between theory and observations of canonical and and He-enriched HB stars. The use of far-UV and optical bands improve the sensitivity, since EHB stars are the brightest objects in the former bands. However, the comparison with theory and/or with empirical templates might be affected by uncertainties in the reddening correction in the far-UV (Dalessandro et al. 2010). It is worth mentioning that the HB morphology of several GCs, including the more massive ones, show gaps, thus affecting comparisons with theory. However, there are two secondary interesting features worth being discussed. *i)*– More massive HB models display more extended blue noses. This evidence, taken at face value, would imply that massive HB structures can cross the RR Lyrae instability strip, thus affecting their pulsation properties (Marconi et al. 2010, in preparation). *ii)*– The central He-burning lifetimes of He-enriched structures are longer than HB models with canonical He content. The difference among EHB structures is clear, and indeed after 100 Myr they did not approach the end of the central helium burning phase.

In order to investigate this point in more detail Fig. 6 illustrates the central helium burning lifetimes for the same HB models plotted in Fig. 5. Predictions plotted in this figure provide a more quantitative estimate of the He-burning lifetime of canonical and He-enriched HB models. The difference with the most helium enriched models ranges from 10% to 30% for ZAHB temperatures larger than logTe≈4.3, i.e. the region of EHB stars. The increase in the lifetime is mainly caused by the fact that they are fainter, since the He-core of He-enhanced models is slightly smaller than the canonical ones. In these structures, the H-shell plays a marginal role, since the envelope mass is quite small. The HB region in which the H-shell becomes relevant in the energy budget is for effective temperatures cooler than logTe≈4.3, and indeed in this region He-enhanced structures are brighter than canonical ones. However, the He-burning lifetime of helium enhanced models is systematically longer over the entire temperature range. The difference is smaller and appears counter-intuitive, since the former structures are, at fixed effective temperature, not only brighter, but also less massive than the latter ones. The increase in the He-burning lifetime is mainly caused by the fact that the hydrogen-burning shell in the He-enriched structures is more efficient, due to the increase in the mean molecular weight. The main outcome of the quoted scenario is that in GCs with a 50% of He-enhanced stars, the HB morphology is governed by these structures. This applies not only to EHB and BHB stars, but to a minor extent also to RHB stars.

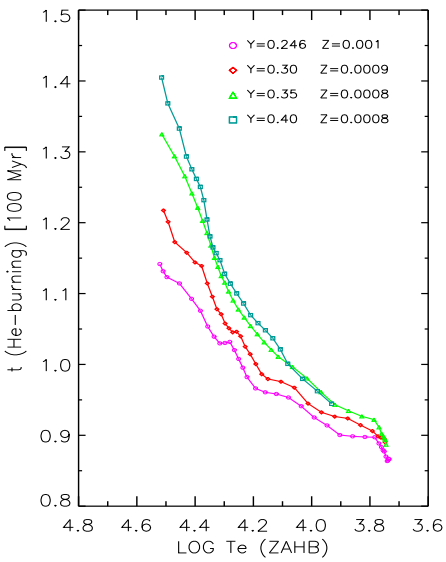

Fig. 6. Central helium burning lifetimes (in units of 100 Myr) as a function of the ZAHB effective temperature for the same models plotted in Fig. 5. The lifetimes were slightly smoothed.

3.2. New routes

Two independent methods appear very promising to constrain the evolutionary history of cluster HB stars. Evolutionary models indicate that HB structures which ignite helium along the white dwarf cooling sequence (*late hot helium flashers*) experience a significant mixing (Sweigart 1997; Brown et al. 2001, 2010; Cassisi et al. 2003, 2009; Miller Bertolami et al. 2008) between the core (helium and carbon-rich) and the envelope (hydrogen rich). The aftermaths of this flash-mixing phenomenon are structures showing a significant increase in the surface abundance of carbon ranging from 1% to 5% and an even more relevant increase in helium content. This is a crucial observable, since the progeny of the helium-enriched scenario is not supposed to be carbon-enriched (see Moehler in these proceedings). In a recent spectroscopic investigation of extreme HB stars in ω Centauri, Moehler et al. (2007); Moehler (2010) found that among the EHB stars ($Te \geq 30,000$ K) roughly the 30% are helium-poor, while the 70% have either solar or super-solar helium abundances. Interestingly enough, the carbon-rich stars are also helium-rich stars, thus supporting the evidence that a fraction of these stars are the aftermath of the *hot helium flasher* scenario. However, more deep and accurate data are required to constrain the fraction of carbon and helium-rich stars and the impact of current evolutionary prescriptions (convective mixing, element diffusion, mass loss, Miller Bertolami et al. 2008).

The first variable extreme horizontal branch star has been recently discovered in ω Cen (Randall, Calamida & Bono 2009). The period is short (114 s) and the luminosity amplitude is ≈0.3 mag. The optical colors indicate for this object an effective temperature of 31,500±6300 K, thus suggesting that it is located inside the instability strip for rapidly oscillating B subdwarfs. This discovery was soundly supported by the identification of three plus one new variable EHB stars in the same cluster (see colored symbols in Fig. 7), using accurate B-band time series data collected with EFOSC at NTT (Randall, Calamida & Bono 2009, 2010). The identification of these objects in a GC is relevant to constrain the evolutionary properties of this new group of variable stars, since up to now pulsating SdB/SdO have only been detected in the field. The astroseismic investigations of the quoted objects appear very promising, since the comparison between observed and predicted frequency pattern can provide optimal estimates, not only of the core mass, but also of the abundance pattern and of the mass of the envelope (van Grootel et al. 2008; Randall, Calamida & Bono 2010). These three structural parameters are crucial to constrain their evolutionary history.

Another interesting aspect concerning the identification of variable EHB stars in a GC is that their properties can help to shed new light on a longstanding open problem concerning the occurrence of binaries among EHB stars (Castellani et al. 2006). Detailed spectroscopic investigations indicate that the fraction among field sdB stars range from 40% (Napiwotzki

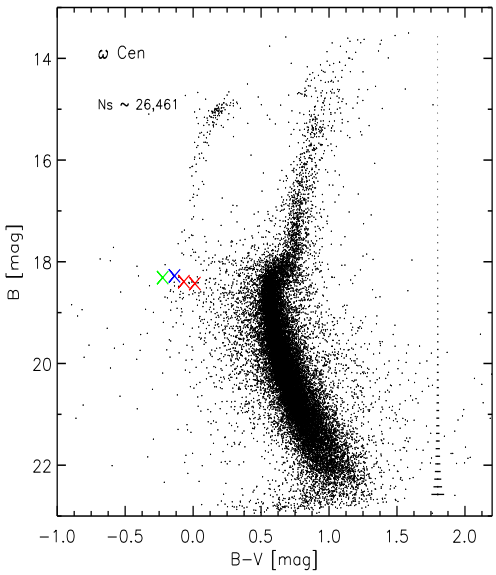

Fig. 7. B,B-V CMD of ω Centauri based on B-band time series data collected with EFOSC at NTT. The colored crosses show the position of the four candidate variable EHB stars. The fourth object has been recently discovered (Randall, Calamida 2010, private communication). The error bars on the right display intrinsic photometric error both in magnitude and in color.

2006) to 60% (Maxted et al. 2001). Moreover, radial velocity measurements indicate that approximately the 50% of them are close binaries with period shorter than a dozen of days (Morales-Rueda et al. 2004, 2006; Heber 2009). On the other hand, up to now there has been no clear identification of binaries among cluster EHB stars (Moni Bidin et al. 2008). In particular, it is not clear whether this finding is the consequence of a difference in their formation channel (Han et al. 2002; Han 2008), or the aftermath of an observational bias.

Finally, we mention that rotation can also play a fundamental role in the evolution of HB stars. However, the empirical and the theoretical rotational scenarios are far from being settled. Detailed radial velocity measurements of field and cluster EHB and BHB indicate that their rotational velocity increases when moving from hotter to cooler effective temperatures. The rotational velocity attains a constant value, smaller than 10 km sec^{-1} for $\log Te \lesssim 4$, and becomes of the order of 20-30 km sec^{-1} for $4 < \log Te \lesssim 3.9$ (Behr 2003; Recio-Blanco et al. 2004). Plain physical arguments suggest that RR Lyrae stars should have rotational velocities larger than 10 km sec^{-1}, but observations indicate that they have smaller rotational velocities. This is the so-called *Peterson conundrum* (Peterson, Rood & Crocker 1995; Peterson, Carney & Latham 1996) and the interested reader is refereed to Preston (2010) for a more detailed discussion. The rotational velocity can also be a good candidate for the second parameter(s) problem in driving the HB morphology (Renzini 1977; Castellani et al. 1980; Catelan, Valcarce & Sweigart 2010).

The period change rate of RR Lyrae stars is also a robust diagnostic to constrain the intrinsic properties of HB stars, and in particular, to establish the evolutionary direction (Rosino 1973; Sweigart & Renzini 1979). The period derivative should be positive for stars evolving from the blue to the red, and negative if the star is evolving from the red to the blue. Note that this difference is crucial to constrain the Oosterhoff dichotomy (Bono et al. 1997), and to constrain the possible occurrence of evolved helium-rich RR Lyrae stars (Marconi et al. 2010, in preparation). Evolutionary prescriptions indicate that He-rich HB structures cross the RR Lyrae instability strip from the blue to the red, at higher luminosities and with smaller mass values when compared with canonical HB models. In a recent investigation, Kunder et al. (2010) found, by using detailed data for a sizable sample of RR Lyrae stars in IC4499, that the observed period change rates are on average one order of magnitude larger than predicted from canonical HB models. This result further supports previous findings on the period derivative in other clusters (Lee & Carney 2010; Jurcsik et al. 2001, 2010) and field (Le Borgne et al. 2007) RR Lyrae stars. The new interesting point is that as empirical estimates on the uncertainties of period change rates are becoming systematically smaller, a stark discrepancy between theory

and observations is found. In turn, this leads to the need for a new spin in pulsation and evolutionary models of RR Lyrae stars.

Finally, we mention what seems to be the most promising route concerning future use of field and cluster RR Lyrae stars as cosmological beacons. In a recent paper, (Preston 2009) brought to attention the identification of both HeI and HeII emission and absorption lines in field RR Lyrae stars. The lines show up during the rising branch of RR Lyrae stars and appear to be the consequence of the shock propagation soon after the phases of minimum radius (Christy 1966; Bono & Stellingwerf 1994; Chadid et al. 1996; Fokin et al. 1999). The idea is not new and dates back to Wallerstein (1959), who detected helium emission lines in his seminal investigation on type II Cepheids. The possibility of a direct measurement of helium lines in RR Lyrae stars appears very promising to constrain this fundamental cosmological parameter. The key advantage of RR Lyrae stars, when compared with similar detections of helium lines in extreme HB stars (Behr 2003) is that they have an extended convective envelope, and therefore they are minimally affected by gravitational settling and/or radiative levitation (Michaud et al. 2004).

4. Cluster white dwarfs

The transition from the HB to the AGB has been discussed in detail by Wood (2010, and references therein). The evolutionary properties of white dwarfs have been discussed by Prada Moroni (2010); Althaus (2010a, and references therein), while WD atmosphere models have been discussed by Koester (2010, and references therein). The interested reader is also referred to the thorough recent reviews by Koester & Chanmugam (1998); Hansen & Liebert (2003); Hansen (2004); Moehler & Bono (2008); Salaris (2008); Kalirai & Richer (2010). In the following, we will focus our attention on the astrophysical use of the WD cooling sequence in GCs. The interested reader is referred to Moehler & Bono (2008) for a comprehensive discussion.

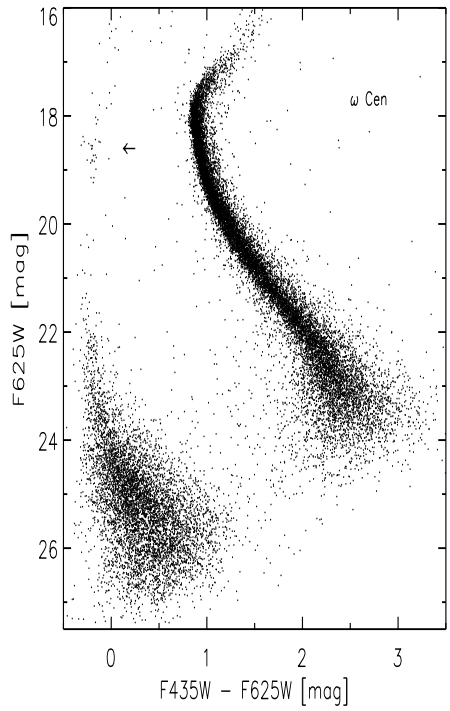

Fig. 8. Optical Color Magnitude Diagram – F625W,F435W-F625W– of ω Centauri (Calamida et al. 2008). Data were collected with ACS-WFC on board the Hubble Space Telescope. The left black arrow marks the position of extreme HB stars. The WD cooling sequence shows up as a well defined region on the left hot faint corner of the CMD. This is the first GC with a number of WDs, which is almost a factor three larger than the number of HB stars.

Among the Galactic GCs, ω Cen is the most massive one. Therefore, the identification by Monelli et al. (2005) of more than 2,000 WD candidates, in three out of the nine ACS@HST pointings located across the cluster center, did not came as a surprise. On the basis of this evidence Monelli et al. (2005) suggested that a fraction of them might be helium-core WDs, since their cooling time scale is slower than canonical CO-core WDs (Castellani et al. 2006; Althaus 2010a). Note that in a Hubble time He-core WDs can only be the aftermath of a binary evolution. These re-

sults were supported by (Calamida et al. 2008) who found, using eight out of nine pointings[2], approximately 6,500 WD candidates. Moreover, they found that the ratio between WD and main sequence (MS) star counts is ≈ a factor of two larger than the ratio between the CO-core WD cooling time and the MS lifetime. This evidence indicates that a fraction of He-core WDs ranging from 10% to 80%, according to their mean mass, can account for the discrepancy between theory and observations.

This finding was recently supported in an independent investigation by (Cassisi et al. 2009). They found that in ω Cen a fraction (∼15%) of suspected He-rich HB stars are not present in the CMD. This missing population could be the progeny of the RGs that does not approach the tip of the RGB and does not ignite central He-burning. Therefore, these stellar structures end up their evolution as He-core WDs, as suggested by Castellani et al. (2006) and by Calamida et al. (2008).

The possible occurrence of He-core WDs in GCs, was also supported by Strickler et al. (2009), by using deep and accurate multiband HST photometry of the nearby GC NGC6397. They found that a group of WDs are, at fixed color, brighter than typical CO WDs and also show strong H_α absorption lines. The theoretical and the observational scenario is far from being settled, and indeed Prada Moroni & Straniero (2009) also suggested that progenitors with stellar masses ranging from 1.8 to 3 $M_\odot$ experiencing a significant mass loss during hydrogen buning phases end up their evolution as low-mass ($0.33 \leq M/M_\odot \leq 0.5$) CO-core WDs. However, the cooling time of He-core WDs is longer than low-mass CO-core Wds, since the former have a higher specific heat.

The data plotted in Fig. 8 make sense to a simple prediction. Assuming that 12 Gyr is the typical age of a GC and a Salpeter-like initial mass function ($\alpha = 2.35$), one finds that the number of cluster WDs is about a factor of 300 larger than the number of HB stars (Brocato, Castellani & Romaniello 1999). This number is a lower limit, since it neglects the fraction of WDs produced in binaries. The current number of HB stars measured in ω Cen is approximately 3,200 (Castellani et al. 2007), thus suggesting that the current sample is a tiny fraction of the entire WD population (≈ 1 million!).

Data plotted in Fig. 9 also contributed to open a new path concerning the astrophysical use of cluster WDs. By using deep ACS-WFC at HST images of of NGC 6397 Hansen et al. (2007); Richer et al. (2008) firmly detected, for the first time, the blue turn of cluster WDs. This evolutionary feature is caused by both steady increase in the stellar mass along

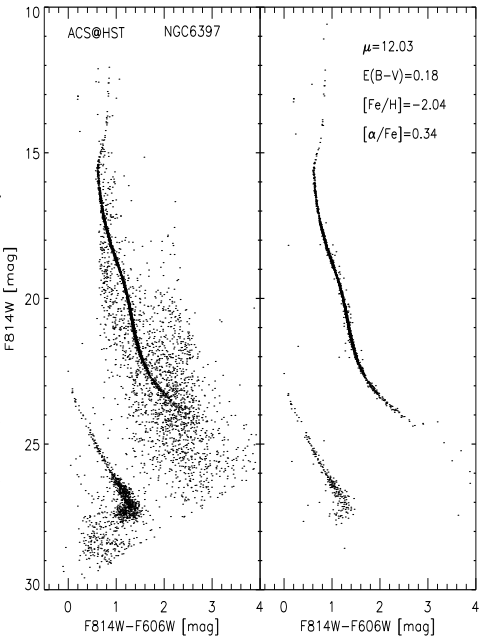

Fig. 9. Left – Deep and accurate F814W,F606W-F814W CMD of NGC 6397 (Richer et al. 2008). Data were collected with ACS-WFC on board the Hubble Space Telescope and the total exposure is roughly 50 hours. This is the first GC for which the optical photometry clearly detected the blue turn in the WD cooling sequence and approached the bottom of the MS. Right – same as the left, but the authors cleaned the cluster data by using the proper motion.

[2] The central pointing was not included, since the photometry was less accurate due to crowding problems.

the WD cooling sequence and by the collisional induced absorption by H_2 molecules in DA (helium and hydrogen-rich envelope) WDs. The identification is particularly robust, since the authors have been able to separate field and cluster candidates by using accurate proper motion measurements. The comparison between theory and observations provided for this cluster very precise distance modulus (μ= 12.02±0.06 mag) and absolute cluster age (t=11.47±0.47 Gyr, Hansen et al. 2007).

4.1. New routes

Whenever either a new instrument, a new wavelength region, or a new observing facility becomes available we are at the classical crossroads: *i)*– improve the precision of well known diagnostics; *ii)*– develop new diagnostics. The latter route is less trivial, but offers a relevant reward: the opportunity to identify new evolutionary features which can provide independent checks on the systematics affecting well established distance and age indicators. Along this path moves the bending that low-mass main sequence stars show in the NIR CMDs (Bono et al. 2009). This bending is marginally dependent on metallicity, and can be adopted to provide robust estimates of both cluster age and distances.

Cluster age (Richer et al. 2008) and distances (Zoccali et al. 2001) based on WDs, in spite of their intrinsic faintness, have been the fresh turning point on these topics. They bring forward two indisputable positive features: *i)*– they are virtually independent of the metal content; *ii)*– they are the ending point of a significant fraction of stars in globular and open clusters, and their properties provide the opportunity to constrain the input physics adopted in previous evolutionary phases.

The literature concerning pros and cons of WDs as age and/or distance indicators is large and detailed. In the following, we briefly mention a few positive features in using deep NIR Color-Magnitude Diagrams of GGCs. Fig. 10 shows a complete predicted CMD, including not only hydrogen burning phases (cluster isochrones), but also helium burning phases (ZAHB) and the WD cooling

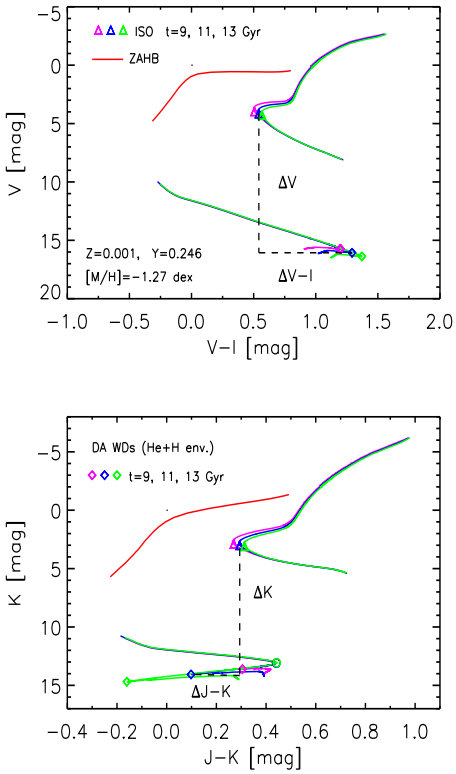

Fig. 10. Top – Predicted V,V-I CMD for metal-intermediate stellar structures. The pink, blue and green solid lines show cluster isochrones at fixed chemical composition (see labeled values) and ages of 9,11 and 13 Gyr. The triangles mark the Main Sequence Turn-Off (MSTO). The red solid line shows the Zero-Age-Horizontal-Branch for the same chemical composition and progenitor mass of M=0.8$M_{\odot}$. right, V,V-J and V,V-K CMDs of NGC 3201. The almost linear pink, blue and green solid lines display the cooling sequences of DA (helium and hydrogen rich envelope) WDs for the same chemical composition and the same ages of the cluster isochrones. The diamonds mark the WD Blue Turn (WDBT) along the cooling sequence. The dashed lines show the difference in magnitude and in color between the MSTO and the WDBT. Bottom – Same as the top, but in the NIR K,J-K CMD. Note that the difference in magnitude and in color is now between the MSTO and the WD Red Turn.

sequences. The key advantages of the models plotted in this figure consist in the fact that they come from a homogeneous theoretical framework (Salaris et al. 2010). Evolutionary models were constructed by assuming the same α-enhanced metal-intermediate chemical composition ([M/H]=-1.27 dex). The cluster isochrones and the WD cooling sequences cover the same age range, i.e. 9,11,13 Gyr. The WD cooling sequences account for the release of gravitational energy, associated with the phase separation of the CO mixture upon crystallization (Stevenson 2010). The chemical composition of the envelope of the quoted DA models is made of helium (0.01 M_{WD}) and hydrogen (0.0001 M_{WD}).

Models plotted in the top panel of Fig. 10 indicate that the difference, both in color and in magnitude, between the Main Sequence turn-off (MSTO) and the WD Blue Turn (WDBT) are strong age indicators. The key advantage of this approach, when compared with traditional methods (CMD fit, luminosity function), is threefold: *i)*– the difference in magnitude and in color is independent of both distance and reddening; *ii)*– it is minimally affected by uncertainties in the photometric zero-point; *iii)*– it is also minimally affected by limits in completeness in the faint limiting magnitude, as soon as the WDBT can be unambiguously identified.

Models plotted in the bottom panel of Fig. 10 appear even more promising in the application of this method. As a matter of fact, WD cooling sequences show in the NIR bands a significant blue turn, due to the collisional-induced-absorption (CIA) of H_2 molecules and soon after a Red Turn (WDRT). A similar feature was already found in old DA WD cooling sequences by Salaris et al. (2000), and is the consequence of an interplay between the occurrence of CIA (strongly affected by surface gravity) and total mass (see their figures 4 and 5). It is worth mentioning, that in this plane an increase in age makes the WDRT bluer, while the MSTO becomes redder, thus increasing the sensitivity of the age derivative. Finally, let us mention that the WDBT seems to be age-independent in this age range. This firm evolutionary feature only depends on the initial-to-final mass (M_i/M_f) ratio (Kalirai et al. 2009a; Salaris et al. 2010, and references therein), therefore, the difference in color between the WDBT and the WDRT is also a robust age indicator (Bono et al. 2010, in preparation).

In passing, we may also note that the minimal dependency of the WD cooling sequence on the metal content and the nature of the physical mechanism causing the WDBT (CIA of H_2 molecules) make this intriguing evolutionary feature a very promising feature in order to constrain either the (M_i/M_f) ratio or the cluster distance.

The WD models plotted in Fig. 11 are the same as in Fig. 10, but the chemical composition of their envelope is typical of DB WDs, i.e. they are only made of helium ($10^{-3.5}$ M_{WD}). As expected, the WD cooling sequences do not show significant either blue or red turns. However, the difference in magnitude between the MSTO and the WD cooling sequence, at the same color of the MSTO, can still be adopted to estimate the cluster age. Note that an increase in age makes the MSTO redder, the same applies to the DB WD cooling sequence, therefore, the age derivative becomes less sensitive. The above evidence might not be severe limit in the application of the new method, since current spectroscopic investigations indicate that a significant fraction of bright cluster WDs are of DA type, i.e. with a helium and hydrogen-rich envelope (Moehler et al. 2004a; Davis et al. 2009).

5. Final remarks

Our knowledge of the advanced evolutionary phases of low-mass stars has significantly improved during the last few years. From an observational point of view, the new results mainly rely either on large photometric and spectroscopic ground-based surveys, or on HST observations (Moehler & Bono 2008). The Sloan Digital Sky Survey identified ≈20,000 WDs in the Galactic field, while more than ≈15,000 WDs have been identified in stellar systems with ACS-WFC at HST (see §4, and Bedin et al. 2009, 2010). The same outcome applies for the input physics,

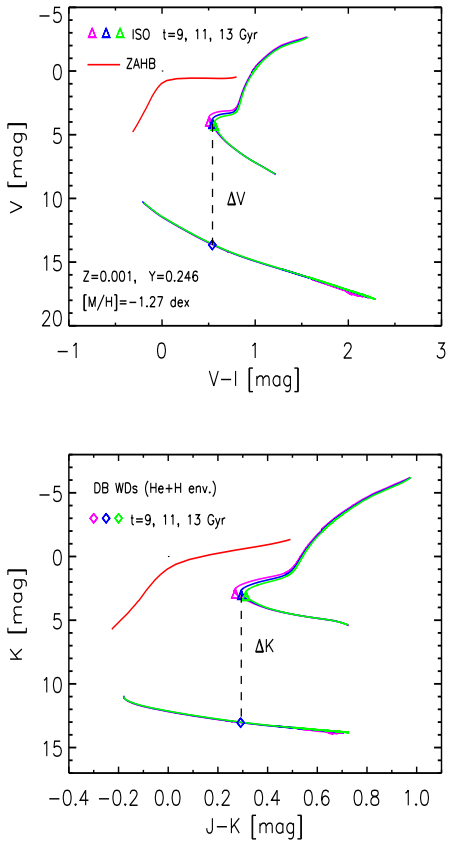

Fig. 11. Same as Fig. 10, but the cooling sequences display predictions for DB (helium-rich envelope) WDs. The vertical dashed line shows the difference in magnitude between the MSTO and the WD cooling sequence at the same color of the MSTO.

currently adopted in constructing WD models (Althaus et al. 2010b; Salaris et al. 2010).

The near future appears even more promising in this field especially if we account for the high sensitivity and spatial resolution of the WFPC3 at HST. A significant quantum jump in the population of field WDs is expected with the Large Synoptic Survey Telescope (LSST)[3]. Preliminary estimates indicate that the number should be of the order of 50 million (Kalirai et al. 2009b).

The astrophysical use of cluster WDs in the NIR bands outlined in section 4.1 are beyond the current limits of ground-based and probably space instrumentation. However, the use of multi-conjugate adaptive optic systems (Marchetti et al. 2006) will provide NIR images with a full width at half maximum (FWHM) of a few hundredths of arcseconds, and a field of view of a few arcminutes squared. This new generation of instruments at the 10m class telescopes are paving the road for the European Extremely Large Telescope (Hook et al. 2006)[4], the Thirty Meter Telescope[5], the Giant Magellan Telescope[6] and the James Webb Space Telescope[7]. The interval of cluster ages we have investigated (9-13 Gyr) indicate that the white dwarf red turn is located between $M_J \sim M_K \sim$ 14–15 mag. If we assume that a 40m class telescope can reach apparent limiting magnitudes of $m_J \sim m_K \sim$ 29–30 mag (Bono et al. 2009), this would imply that we can investigate the GCs within 15 kpc. In passing, we note that the same limiting magnitudes will allow us to investigate HB stars, and, in turn, their morphology not only in GCs, but also ultra compact dwarfs and dwarf ellipticals in nearby galaxy clusters (Hilker 2010).

Certainly we will deal with big challenges not only to properly assess longstanding astrophysical problems, but also in the advancement of new technological enterprises. These appealing opportunities further support the evidence that cluster WDs in the near future will remain relevant targets for theoretical and empirical investigations.

Acknowledgements. It is a pleasure to thank the several senior colleagues with whom I have the pleasure to collaborate on this exciting field of stellar pulsation and evolution. Among them I would like to mention Filippina Caputo, who is approaching the

[3] http://lsst.org
[4] `http://www.eso.org/projects/e-elt/`
[5] `http://www.tmt.org/`
[6] `http://www.gmto.org/`
[7] http://www.stsci.edu/jwst/

retirement and I would like to thank her for being the promoter of many scientific projects. For me and many other younger students and collaborators it has been a real pleasure to collaborate with her. We all agree that we will keep her busy for many years to come!

I also have a debt of gratitude to the students and young researchers who helped me in fixing the content of this paper (A. Calamida, M. Dall'Ora, A. Di Cecco, M. Fabrizio, E. La Gioia, M. Monelli, S. Randall, L. Troisi). I thank J. Kalirai and H. Richer for sending me their data on NGC 6397 in electronic form and S. Cassisi, A. Kunder, M. Romaniello, M. Salaris and M. Zoccali for a detailed reading of an early draft of this manuscript and for many useful discussions on advanced evolutionary phases. I apologize for having taken advantage of being co-editor of the proceedings. This allowed me to update and in several cases to change the original version of this manuscript before the publication. I also acknowledge support from the ESO Visitor program. This work was partially supported by PRIN-INAF2010 (P.I.: R. Gratton).

References

Abdo, A. A., Ackermann, M., Ajello, M. et al. 2010, Science, 329, 817
Anderson, J. 2002, ASPC, 265, 87
Albrow, M. D., et al. 2001, ApJ, 559, 1060
Aller, L. H. & McLaughlin, D. B. (ed.) 1965, Stellar Structure - Stars and Stellar Systems (Chicago: Univ. of Chicago press)
Althaus, L. G. 2010a, MemSait, this volume
Althaus, L. G. et al. 2010b, ApJ, 719, 612
Anderhub, H., et al. 2001, ApJ, 559, 1060
Angulo, C., et al. 1999, Nucl. Phys. A, 656, 3
Arp, H. 1955, AJ, 60, 31
Baade, W. 1958, RA, 5, 303
Bedin, L. R. et al. 2004, ApJ, 605, L125
Bedin, L. R. et al. 2009, ApJ, 697, 965
Bedin, L. R. et al. 2010, ApJ, 708, L32
Behr, B. B. 2003, ApJ, 149, 67
Behr, B. B. 2003, ApJS, 149, 101
Blaauw, A. & Schmidt, M. (ed.) 1965, Galactic Structures, (Chicago: Univ. of Chicago press)
Blaauw, A. 1999, Ap&SS, 267, 45
Blaauw, A. 2004, ARA&A, 42, 1
Bono, G., et al. 1995, A&A, 297, 115
Bono, G., Caputo, V., Castellani, V., & Marconi, M. 1997, A&AS, 121, 327
Bono, G., & Stellingwerf, R. F. 1994, ApJS, 93, 233
Bono, G., et al. 2009, in Science with the VLT in the ELT Era, (Netherlands: Springer), 67
Bono, G., Stetson, P. B., VandenBerg, D. A. et al. 2010, ApJ, 708, L74
Boyer, M. L., Skillman, E. D., van Loon, Jacco Th., Gehrz, R. D., & Woodward, C. E. 2009, ApJ, 697, 1993
Brocato, E. Castellani, V., & Romaniello, M. 1999, A&A, 345, 499
Brown, T.M., Sweigart, A.V., Lanz, T., Landsman, W. B., & Hubeny, I. 2001, 562, 368
Brown, T. M., Sweigart, A. V., Lanz, T., Smith, E. et al. 2010, ApJ, 718, 1332
Buonanno, R.; Corsi, C. E.; Zinn, R.; Fusi Pecci, F.; Hardy, E.; Suntzeff, N. B. 1998, ApJ, 501, L33
Buzzoni, A.; Pecci, F. F.; Buonanno, R.; Corsi, C. E. 1983, A&A, 128, 94
Calamida, A., Bono, G., Stetson, P. B. et al. 2007, ApJ, 670, 400
Calamida, A., Corsi, C.E., Bono, G. et al. 2008, ApJ, 673, L29
Cannon, R. D., Croke, B. F. W., Bell, R. A., Hesser, J. E., & Stathakis, R.A. 1998, MNRAS, 298, 601
Carretta, E., Bragaglia, A., Gratton, R. G., Lucatello, S., & Momany, Y. 2007, A&A, 464, 927
Carretta, E., et al. 2009, A&A, 505, 117
Cassisi, S. et al. 2000, MNRAS, 315, 679
Cassisi, S.; Castellani, V.; degl'Innocenti, S.; Salaris, M.; Weiss, A. 1999, A&AS, 134, 103
Cassisi, S., Schlattl, H., Salaris, M., & Weiss, A. 2003, ApJ, 582, L43
Cassisi, S., Salaris, M., Pietrinferni, A. et al. 2008, ApJ, 672,L115
Cassisi, S., Salaris, M., Anderson, J., et al. 2009, ApJ, 702, 1530
Castellani, V., Calamida, A., Bono, G., et al. 2007, ApJ, 663, 1021
Castellani, M., & Castellani, V. 1993, ApJ, 407, 649
Castellani, M., Castellani, V., Prada Moroni, P.G. 2006, A&A, 457, 569
Castellani, V.; Iannicola, G.; Bono, G. et al. 2006, A&A, 446, 569

Castellani, V. et al. 1980, Ap&SS, 73, 11
Catelan, M. 2009, Ap&SS, 320, 261
Catelan, M., Valcarce, A. A. R., & Sweigart, A. V. 2010, in IAUS, Star clusters: basic galactic building blocks throughout time and space, 266, 281
Charbonnel, C. & Lagarde, N. 2010, A&A, 522, 10
Cohen, J. G. 1978, ApJ, 223, 487
Chadid, M., & Gillet, D. 1996, A&A, 308, 481
Chiosi, C., Bertelli, G., Bressan, A. 1992, ARA&A, 30, 235
Chiosi, C. & Maeder, A. 1986, ARA&A, 24, 329
Christy, R. F. 1966, ApJ, 144, 108
Cool, A. M., Piotto, G., King, I. R. 1996, ApJ, 468, 655
Dalessandro, E.; et al. 2010, MNRAS, accepted
D'Antona, F. & Caloi, V. 2008, MNRAS, 390, 693
D'Antona, F., Bellazzini, M., Caloi et al. 2005, ApJ, 631, 868
Davis, D. S., et al. 2009, ApJ, 705, 398
Decressin, T., Meynet, G., Charbonnel, C., Prantzos, N., & Ekstrm, S. 2007, A&A, 464, 1029
Denissenkov, P. A., & Weiss, A. 2004,ApJ, 603, 119
Di Criscienzo, M., Caputo, F., Marconi, M., & Musella, I. 2006, MNRAS, 365, 1357
D'Cruz, N.L., Dorman, B., Rood, R. T. 1996, ApJ, 466, 359
Dieball, A. et al. 2007, ApJ, 670, 379
Eggen, O. J., Lynden-Bell, D., Sandage, A. R. 1962, ApJ, 136, 748
Ferguson, J. W. et al. 2005, ApJ, 623, 585
Fokin, A. B., Gillet, D., & Chadid, M. 1999, A&A, 344, 930
Freire, P. C. C. et al. 2008, ApJ, 675, 670
Galleti S., et al. 2004, A&A, 416, 917
Gratton, R. G., Bonifacio, P., Bragaglia, A., Carretta, E. et al. 2001, A&A, 369, 87
Gratton, R., Sneden, C., & Carretta, E. 2004, A&A, 42, 385
Greenstein, J. L. (ed.) 1960, Stellar Atmospheres (Chicago: Univ. of Chicago press)
Greggio, L., & Renzini, A. 1990, ApJ, 364, 35
Han, Z. 2008, A&A, 484, 31
Han, Z., Podsiadlowski, P., Maxted, P.F.L., Marsh, T.R., Ivanova, N., 2002, MNRAS, 336, 449
Hansen, B. M. S., PhR, 399, 1
Hansen, B. M. S. & Liebert, J. 2003, ARA&A, 41, 465
Hansen, B. M. S. et al. 2007, ApJ, 671 380
Harbeck, D., Grebel, E. K., & Smith, G. H. 2003, ANS, 324, 78
Harris W. E. 1996, AJ, 112, 1487
Harris W. E. 2009, ApJ, 699, 254
Heber, U. 2009, ARA&A, 47, 211
Heinke, C. O. et al. 2010, ApJ, 714, 894
Hilker, M. et al. 2010, A Universe of Dwarf Galaxies: Observations, Theories, Simulations, eds. M. Koleva, P. Prugniel & I. Vauglin, in press, arXiv1010.3023
Hook, I., Dalton, G., Gilmozzi, R. et al. 2006, SPIE, 6267, 69
Hoyle, F. 1959, MNRAS, 119, 124
Iannicola, G., Monelli, M., Bono, G. et al. 2009, ApJ, 696, L120
Iben,I., & Rood,R.T. 1969, Nature, 224, 1006
Iglesias, C. A., & Rogers, F. J. 1996, ApJ, 464, 943
Jurcsik, J., Clement, C., Geyer, G.H., & Domsa, I. 2001, AJ, 121, 951
Jurcsik, J., et al. 2010, MNRAS, accepted, arXiv1010.1119
Kalirai, J. S., & Richer, H. B. 2010, RSPTA, 368, 755
Kalirai, J. S. et al. 2008, ApJ, 676, 594
Kalirai, J. S. et al. 2009, ApJ, 705, 408
Kalirai, J. S. et al. 2009, astro2010S.147
King, J. R. et al. 1998, AJ, 115, 666
Koester, D. 2010, MemSait, this volume
Koester, D. & Chanmugam, G. 1990, RPPh, 53, 837
Kraft, R.P.1979, ARA&A, 17, 309
Kraft, R. P. 1994, PASP, 106, 553
Kraft, R. P. 2009, ARA&A, 47, 1
Kunder, A., et al. 2010, AJ, accepted, arXiv:1010.5794
Le Borgne, L.F., et al. 2007, A&A, 476, 307
Lee, W. H., Ramirez-Ruiz, E., & van de Ven, G. 2010, ApJ, 720, L953
Lee, J. & Carney, B. W. 1999, AJ, 118, 1373
Leep, Wallerstein, & Oke 1986, AJ, 91, 1117
Maeder, A. & Meynet, G. 2000, ARA&A, 38, 143

Maeder, A., & Meynet, G. 2006,A&A, 448, L37
Marchetti, E., et al. 2006, SPIE, 6272, 21
Marks, M. & Kroupa, P. 2010, MNRAS, accepted, arXiv:1004.2255
Marigo, P. & Girardi, L. 2007, A&A, 469, 239
Marigo, P., Girardi, L., Bressan, A., Groenewegen, M. A. T. et al. 2008, A&A, 482, 883
Maxted, P.F.L., Heber, U., Marsh, T.R., North, R.C. 2001, MNRAS, 326, 1391
Michaud, G., Richard, O., Richer, J., VandenBerg, D. A. 2004, ApJ, 606, 452
Miller Bertolami, M. M., Althaus, L. G., Unglaub, K., & Weiss, A. 2008, A&A, 491, 253
Milone, A. P., et al. 2008, ApJ, 673, 241
Moehler, S. 2010, MemSait, this volume
Moehler, S. & Bono, G. 2008, in White Dwarfs, (Springer, ASSL), in press, arXiv:0806.4456v2
Moehler, S. et al. 2004a, A&A, 415, 313
Moehler, S.; Sweigart, A. V.; Landsman, W. B.; Hammer, N. J.; Dreizler, S. 2004b, A&A, 415, 313
Moehler, S., Dreizler, S., Lanz, T., Bono, G., et al. 2007, A&A, 475, L5
Monelli, M., Corsi, C.E., & Castellani, V. et al. 2005, ApJ, 621, L117
Moni Bidin, C., Catelan, M., Altmann, M., 2008, A&A, 480, 1
Morales-Rueda, L., Maxted, P.F.L., Marsh, T.R. 2004, Ap&SS, 291, 299
Morales-Rueda, L., Maxted, P.F.L., Marsh, T.R. 2006, Balt. Astron. 15, 187
Napiwotzki, R. A&A, 451, 27
Norris, J., Cottrell, P. L., Freeman, K. C., Da Costa, G. S. 1981, ApJ, 244, 205
Norris, J. E. 2004, ApJ, 621, L57
O'Connell, D.J.K. ed. Stellar Populations (Amsterdam: North Holland Publishing)
Ortolani, S.,& Rosino, L. 1987, A&A, 185, 102
Osborn, W. 1971, The Observatory, 91, 223
Osterbrock, D. E. 2003, in 'Walter Baade : a life in astrophysics', (Princeton: Princeton Univ. Press).
Penev, K. Barranco, J. Sasselov, D. 2009, ApJ, 705, 285
Peterson, R. C. 1980, ApJ, 237, L87
Peterson, R. C., Rood, R. T., & Crocker, D. A. 1995, ApJ, 453, 214
Peterson, R. C., Carney, B. W., & Latham, D. W. 1996, ApJ, 465, L47
Prada Moroni, P. G. & Straniero, O. 2009, A&A, 507, 1575
Prada Moroni, P. G. 2010, MemSait, this volume
Pietrinferni, A., Cassisi, S., Salaris, M., Castelli, F. 2004, ApJ, 612, 168
Pietrinferni, A., Cassisi, S., Salaris, M., Castelli, F. 2006, ApJ, 642, 797
Pilachowski, C. A., Sneden, C., & Wallerstein, G. 1983, APJS, 52, 241
Piotto, G., Bedin, L. R., Anderson, J. et al. 2007, ApJ, 661, L53
Potekhin, A. Y., Chabrier, G., & Shibanov, Y. A. 1999, Phys. Rev. E, 60, 2193
Prantzos, N., & Charbonnel, C. 2006, A&A, 458, 135
Preston, G. W. 2009, A&A, 507, 1621
Preston, G. W. 2010, submitted to AJ, arXiv1008.4618
Randall, S. K., Calamida, A., & Bono, G. 2009, A&A, 494, 1053
Randall, S. K., Calamida, A., & Bono, G. 2009, CoAst, 159, 88
Randall, S. K., Calamida, A., & Bono, G. 2010, 2010, Ap&SS, 329, 55
Ramirez, S. V., & Cohen, J. G. 2002, AJ, 123, 3277
Renzini, A. 1977, in Saas-Fee Advanced Course 7, Advanced Stages in Stellar Evolution, Edited by P. Bouvier & A. Maeder
Renzini, A. 2008, MNRAS, 391, 354
Recio-Blanco, A., Piotto, G., Aparicio, A., & Renzini, A. 2004, A&A, 417, 597
Richer, H. B. et al. 2008, AJ, 135, 2141
Richer, H. B., & Fahlman, G. G. 1988, ApJ, 325, 218
Rogers, F. J. & Nayfonov, A. 2002, ApJ, 576, 1064
Rood, R. & Iben, I., Jr. 1968, ApJ, 154, 215
Rosino, L. 1973, ASSL, 36, 51
Schlattl, H. & Salaris, M. 2003, A&A, 402, 29
Salaris, M. 2008, in IAU Symposium, The Ages of Stars, 258, 287
Salaris, M. et al. 2000, ApJ, 544, 1036

Salaris, M. et al. 2010, ApJ, 716, 1241
Sandage, A. 1953, AJ, 58, 61
Sandage, A. 1962, ApJ, 135, 349
Sandage, A. 1990, JRASC, 84, 70
Sandage, A. 2007, in 'The Mount Wilson Observatory: Breaking the Code of Cosmic Evolution', (Cambridge: Cambridge Univ. press)
Sandquist, E.L., & Martel, A.R.2007, ApJ, 654, L65
Shapley,H. 1928, Nature, 122, 482
Shen, Z. -X., Bonifacio, P., Pasquini, L., & Zaggia, S. A&A, accepted, 2010arXiv1011.1718
Schwarzschild, M., Howard, R., Harm, R. 1957, ApJ, 125, 233
Siegel, M. H., et al. 2007, ApJ, 667, L57
Smith, G. H. 1987, PASP, 99, 67l
Strassmeier, K. G. et al. 2010, A&A, 520, 52
Stevenson, D. J. 1977, PASAu, 3, 167
Strickler, R. R., Cool, A. M., Anderson, J., et al. 2009, ApJ, 699, 40
Suntzeff, N. B., & Smith, V. V. 1991, ApJ, 381, 160
Sweigart, A. V. 1997, ApJ, 474, L23
Sweigart, A. V. & Renzini, A. 1979, A&A, 71, 66
Thompson, I. B. et al. 2010, AJ, 139, 329
Thoul, A. A., Bahcall, J. N., & Loeb, A. 1994, ApJ, 421, 828
Valenti, E., Ferraro, F. R., & Origlia, L. 2007, AJ, 133, 1287
van Grootel, V. 2008, A&A, 488, 685
VandenBerg, D. A., Casagrande, L. & Stetson, P. B. 2010, AJ, 140, 1020
VandenBerg, D. A., Bergbusch, P. A., Dowler, P. D. 2006, ApJS, 162, 375
VandenBerg, D. A., Edvardsson, B. Eriksson, K. Gustafsson, B. 2008, ApJ, 675, 746
Ventura, P., D'Antona, F., Mazzitelli, I., & Gratton, R. 2001, ApJ, 550, L65
Ventura, P.; Marigo, P. 2010, MNRAS, 408, 2476
Ventura, P., Zeppieri, A. Mazzitelli, I., D'Antona, F. 1998, A&A, 334, 953
Villanova, S., Piotto, G., & Gratton, R. 2009, A&A, 499, 755
Vink, J. S. & Cassisi, S. 2002, A&A392, 553
Wallerstein, G. 1958, ApJ, 128, 141
Wallerstein, G. 1959, ApJ, 130, 560
Weiss, A. & Ferguson, J. W. 2009, A&A, 508, 1343
Wood, P. R., Whiteoak, J. B., Hughes, S. M. G., Bessell, M. S. et al. 1992, ApJ, 397, 552
Wood, P. R. 2010, MemSait, this volume
Woodworth, S. C., & Harris, W. E. 2000, AJ, 119, 2699
Zinn, R. 1985, ApJ, 293, 424
Zoccali, M., et al. 2000, ApJ, 530, 418
Zoccali, M., Renzini, A., Ortolani, S., et al. 2001, ApJ, 553, 733
Zoccali, M., Renzini, A., Ortolani, S. et al. 2003, A&A, 399, 931